Supporting Information

In-situ preparation of Nb-Pb codoped and Pd loaded TiO_2 photocatalyst from waste multi-layer ceramic capacitors by a chlorination-leaching process

Bo Niu[1] and Zhenming Xu[1, 2]*

[1]School of Environmental Science and Engineering, Shanghai Jiao Tong University, 800 Dongchuan Road, Shanghai 200240, People's Republic of China

[2]Shanghai Institute of Pollution Control and Ecological Security, Shanghai 200092, People's Republic of China

Corresponding author:

Zhenming Xu

Tel: +86 21 5474495; Fax: +86 21 5474495;

E-mail: zmxu@sjtu.edu.cn

Photocatalytic performance experiments

The photocatalytic H_2 production experiments were carried out in a quartz device (LabSolar-IIIAG, Perfect Light, China). In a typical experiment, 0.1 g catalyst was dispersed in 100 ml of aqueous solution with 10 vol% triethanolamine (TEOA) as the sacrificial agent. Then, the mixture was transferred into the reactor with a quartz cover. After sealing the reactor, the quartz device was evacuated using a vacuum pump to remove the air in the device. The reactor was illuminated by a 300 W Xe lamp (Perfect-Light, China) with an AM 1.5 cutoff filter as the simulated sunlight source, respectively. Magnetic stirring of the solution was maintained through the experiment. The H_2 evolution was measured by gas chromatography (GC2010plus, Japan, Ar as carrier gas). The recyclable photocatalytic activity tests were also performed, and the photocatalyst was collected by centrifugation after each run and used for next run.

The photocatalytic RhB degradation activities of the samples were also evaluated under simulated sunlight irradiation using a 300 W Xe lamp (Perfect-Light, China) with an AM 1.5 cutoff filter. In a typical run, 0.05 g catalyst was added into 50 mL of RhB solution with the concentration of 10 mg/l. The mixture was magnetically stirred for 60 min in dark to achieve the adsorption-desorption equilibrium. Then, the reaction system was irradiated. During the irradiation, 3 mL of the suspension was collected every 30 min and separated by centrifugation to remove the photocatalyst. The concentration of RhB was determined by a UV-vis spectrophotometer (Perkin-Elmer, USA). The recyclable photocatalytic activity tests were also performed. The

photocatalyst was collected by centrifugation after each run and washed with deionized water several times and dried at 80 ^{o}C for 12 h. Then the dried photocatalyst was used for the next run. In addition, the trapping experiments of the recycled sample with addition of triethanolamine (TEOA, 1 mM), 1, 4-benzoquinone (BQ, 1 mM) and isopropyl alcohol (IPA, 1 mM) for RhB degradation were also conducted to detect the role of active species (h^+, $\bullet O_2^-$, and •OH) in the photocatalytic process. The trapping experiments were like the photodegradation experiment except that a quantity of scavengers was added to the RhB solution prior to adding photocatalyst. All the experiments were performed under ambient conditions.

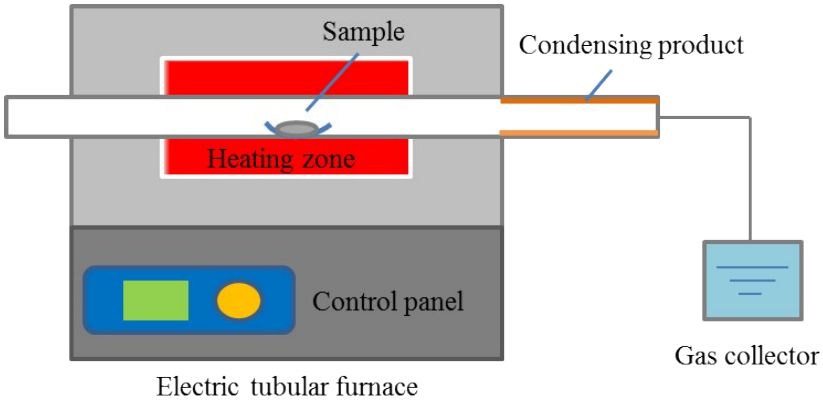

Fig. S1. Schematic diagram of the CM equipment.

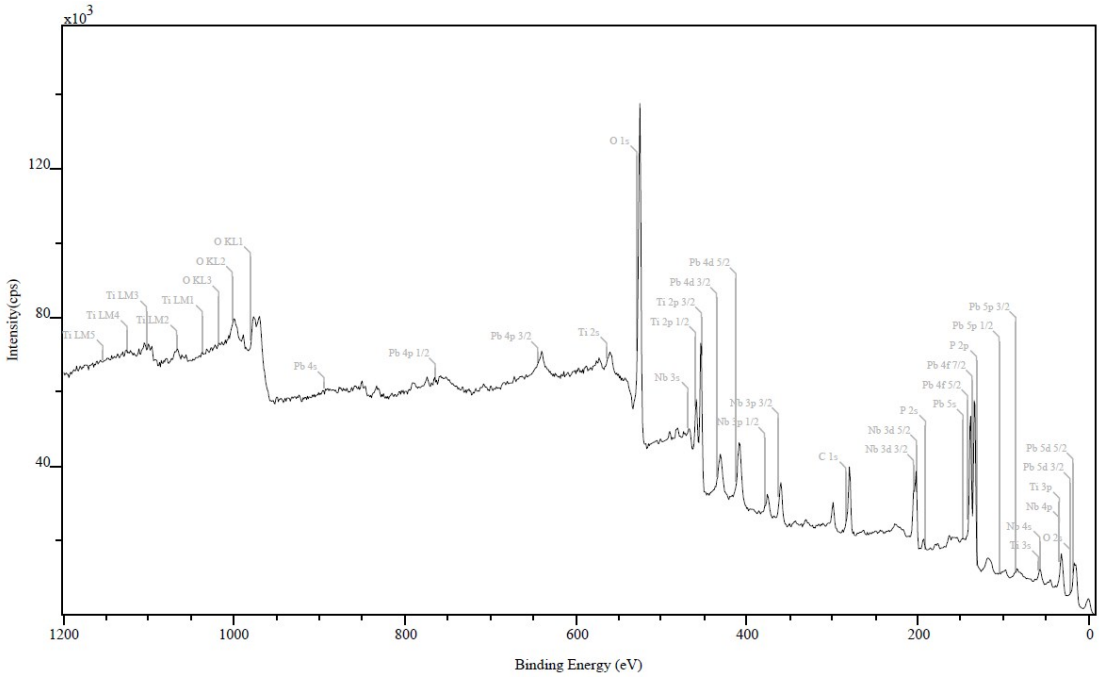

Fig. S2. XPS survey spectra of the recycled sample.

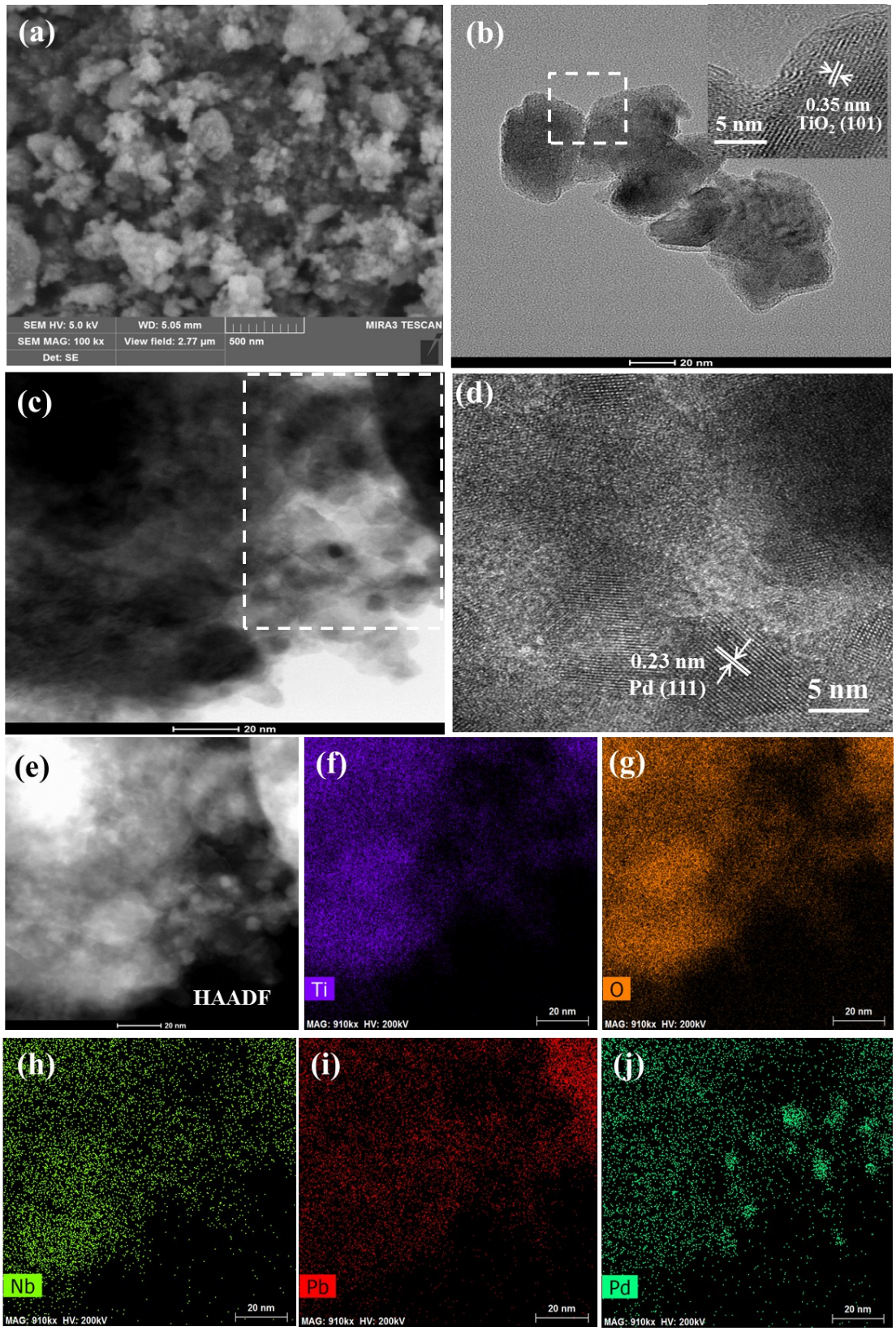

Fig. S3. (a) SEM; (b) and (c) TEM; (d) HR-TEM; (e) HAADF; and (f-j) EDS mapping images of the recycled sample.

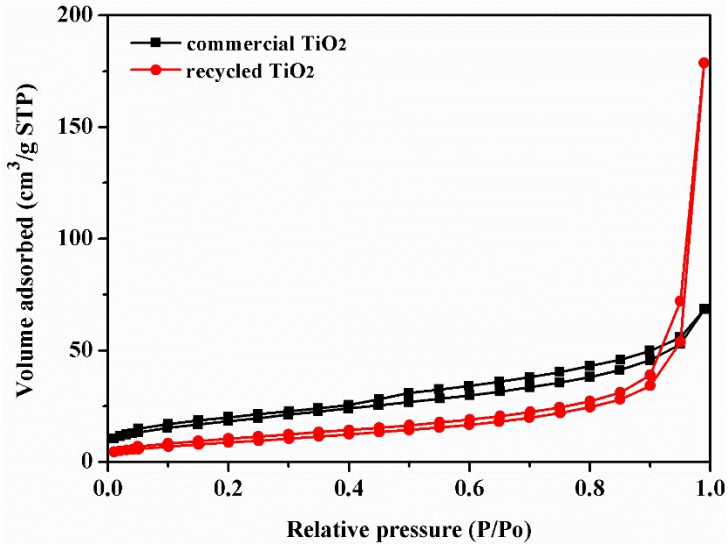

Fig. S4. The nitrogen sorption isotherm curves of the recycled and commercial samples.

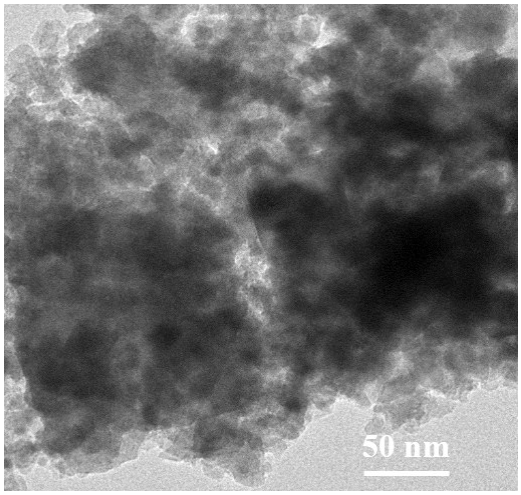

Fig. S5 The TEM image of commercial P25 TiO_2 purchased from MACKLIN reagent.

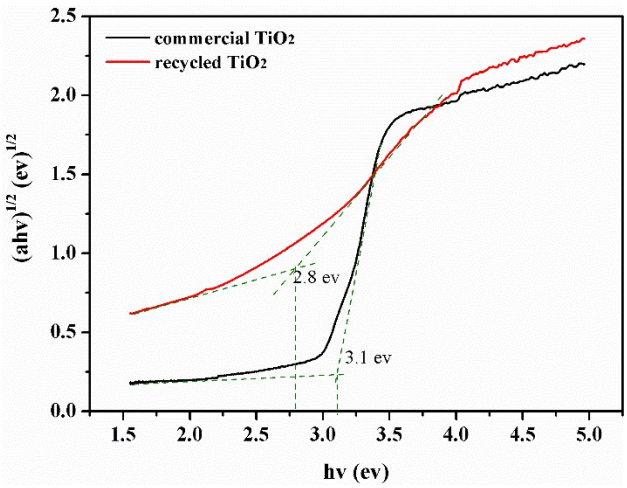

Fig. S6. $(ahv)^{1/2}$ versus photon energy (hv) curves of the recycled and commercial TiO_2.

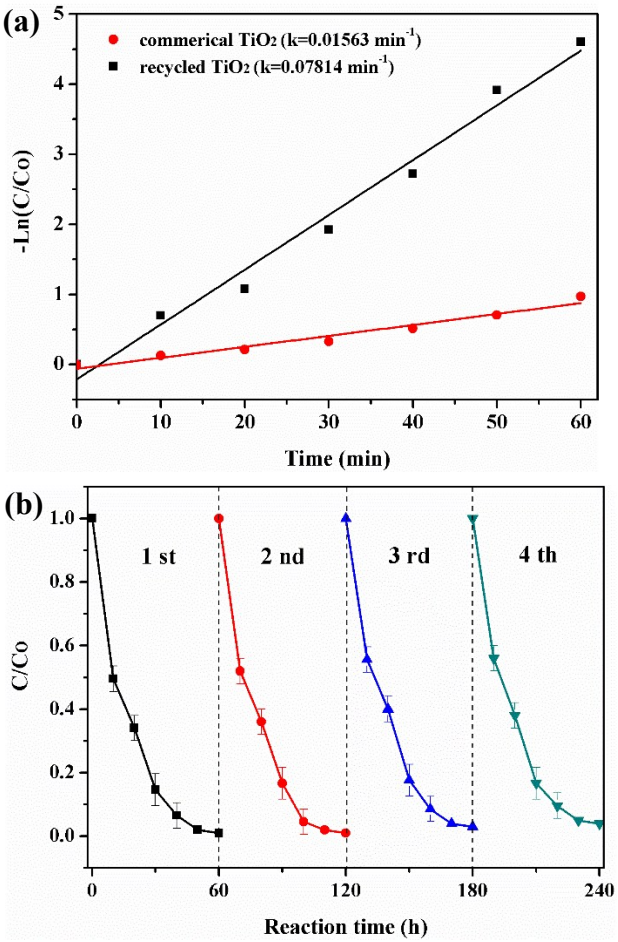

Fig. S7. (a) The chemical kinetics curve for RhB degradation and (b) the cycle runs of the photocatalytic activity of recycled sample for RhB degradation under simulated sunlight irradiation.

Table S1 The composition of the as-prepared samples measured by ICP-MS and the calculated $\bar{X}$ and S

Samples	Composition (%)			
	Ti	Nb	Pb	Pd
0#[a]	39.21	10.88	8.09	1.28
1#	40.13	10.22	7.97	1.19
2#	38.59	10.57	8.22	1.26
3#	38.98	11.24	8.04	1.19
4#	39.41	10.69	7.92	1.15
5#	39.16	11.02	7.95	1.30
6#	39.88	10.91	7.88	1.26
$\bar{X}$ (%)	39.34	10.79	8.01	1.23
S (%)	0.53	0.33	0.12	0.06

Note: 0# is the original sample, and 1-6# are the new six batches.

We applied statistical method (random sampling) to design the experiments to verify the reproducibility of the preparing method in delivering photocatalytic materials. Six batches of waste MLCCs were randomly chosen to be involved in the experiments again. The weight of each batch of waste MLCCs was about 100 g. The composition of as-prepared photocatalysts was analyzed by ICP-MS. Then, the mean ($\bar{X}$) and standard deviation (S) of the composition of the samples were calculated as follows,

$$\bar{X} = \frac{\sum X}{n}$$

$$S = \sqrt{\frac{\sum (X - \bar{X})^2}{n - 1}}$$

The ICP-MS results and calculated $\bar{X}$ and S were listed in **Table S1**. The S value of Ti, Nb, Pb and Pd were 0.53%, 0.33%, 0.12% and 0.06%, respectively, which showed good numeric stability. The results further suggested that the preparation process was repeatable.

Table S2 The H_2 evolution rate and RhB degradation rate of the as-prepared samples and the calculated $\bar{X}$ and S

Sample	0#	1#	2#	3#	4#	5#	6#	$\bar{X}$	S
H_2 evolution rate (μmol/g/h)	185.04	189.01	181.87	182.04	186.45	190.06	187.35	185.97	3.19
RhB degradation rate (min^{-1})	0.07814	0.08122	0.07245	0.07641	0.07984	0.08332	0.08055	0.07885	0.0036

Note: 0# is the original sample, and 1-6# are the new six batches.

Table S3 Recent studies on TiO_2-based photocatalysts for H_2 production

Photocatalyst	H_2-production rate ($\mu mol \cdot g^{-1} \cdot h^{-1}$)	Light source (nm)	Sacrificial reagent	Cocatalyst	Reference (Year)
W/N codoped TiO_2	17.6	λ>400	ethanol	--	[1] (2014)
TiO_2/g-C_3N_4	74.7	Visible light	Methanol	Pt	[2] (2011)
TiO_2/$ZnTiO_3$	192.5	UV light	Ethanol	Pt	[3] (2017)
TiO_2/g-C_3N_4	112	λ>420	Methanol	---	[4] (2016)
TiO_2/CuO	20.3	UV light	Ethanol	--	[5] (2013)
C_{60}-decorated CdS/TiO_2	120.6	λ=420	Na_2S-Na_2SO_3	--	[6] (2015)
Nb-Pb codoped and Pd loaded TiO_2	185.04	simulated sunlight	TEOA	Pd	This work

Table S4 Recent studies on TiO_2-based catalysts for RhB degradation

Photocatalyst	Photocatalytic result	Light source (nm)	Reference (Year)
B-doped TiO_2	2.03 times higher than that of TiO_2	simulated sunlight	[7] (2013)
TiO_2/g-C_3N_4	1.67 times higher than that of TiO_2	λ>400	[8] (2016)
TiO_2/Mn_xO_y	2.37 times higher that of TiO_2	λ>420	[9] (2015)
Gd-dopedTiO_2	2.05 times higher that of TiO_2	Visible light	[10] (2017)
C-doped TiO_2	1.27 times higher than that of TiO_2	Visible light	[11] (2015)
Ag_xAu_{1-x}/TiO_2	10 times higher than that of TiO_2	λ>400	[12] (2015)
V dopedTiO_2/diatomite	7.19 times higher than of TiO_2	simulated	[13] (2015)
Ni/NiO/TiO_2	1.64 times higher than of TiO_2	sunlight	[14] (2018)
Nb-Pb codoped and Pd loaded TiO_2	5 times higher than that of TiO_2	simulated sunlight	This work

References

[1] J. Gong, C. Yang, J. Zhang and W. Pu, Appl. Catal., B 2014, **152-153**, 73-81

[2] H. Yan and H. Yang, J. Alloys Compd., 2011, **509**, L26-L29.

[3] H. Tian, S. Wang, C. Zhang, J.-P. Veder, J. Pan, M. Jaroniec, L. Wang and J. Liu, J. Mater. Chem. A, 2017, **5**, 11615-11622.

[4] Z. Jiang, C. Zhu, W. Wan, K. Qian, J. Xie, J. Mater. Chem. A, 2016, **4**, 1806-1818.

[5] W.T. Chen, V. Jovic, D.S. Waterhouse, H. Idriss and G. I. N. Waterhouse, Int. J. Hydrogen Energy 2013, **38**, 15036-15048.

[6] Z. Lian, P. Xu, W. Wang, D. Zhang, S. Xiao, X. Li and G. Li, ACS Appl. Mat. Interfaces 2015, **7**, 4533-4540.

[7] L. Li, Y. Yang, X. Liu, R. Fan, Y. Shi, S. Li, L. Zhang, X. Fan, P. Tang, R. Xu, W. Zhang, Y. Wang and L. Ma, Appl. Surf. Sci., 2013, **265**, 36-40.

[8] X. Liu, N. Chen, Y. Li, D. Deng, X. Xing and Y. Wang, Scientific reports, 2016, **6**, 39531.

[9] D. Lu, P. Fang, X. Liu, S. Zhai, C. Li, X. Zhao, J. Ding and R. Xiong, Appl. Catal., B 2015, **179**, 558-573.

[10] D. Toloman, A. Popa, M. Stefan, O. Pana, T. D. Silipas, S. Macavei and L. Barbu-Tudoran, Mater. Sci. Semicond. Process., 2017, **71**, 61-68.

[11] Y. Zhang, Z. Zhao, J. Chen, L. Cheng, J. Chang, W. Sheng, C. Hu and S. Cao, Appl. Catal., B 2015, **165**, 715-722.

[12] Y. Zhu, S. Yang, J. Cai, M. Meng and X. Li, Mater. Lett., 2015, **154**, 163-166.

[13] B. Wang, G. Zhang, X. Leng, Z. Sun and S. Zheng, J. Hazard. Mater., 2015, **285**, 212-220.

[14] Q. Zhu, N. Liu, N. Zhang, Y. Song, M. S. Stanislaus, C. Zhao and Y. Yang, J. Environ. Chem. Eng., 2018, **6**, 2724-2732.

DFT calculation results

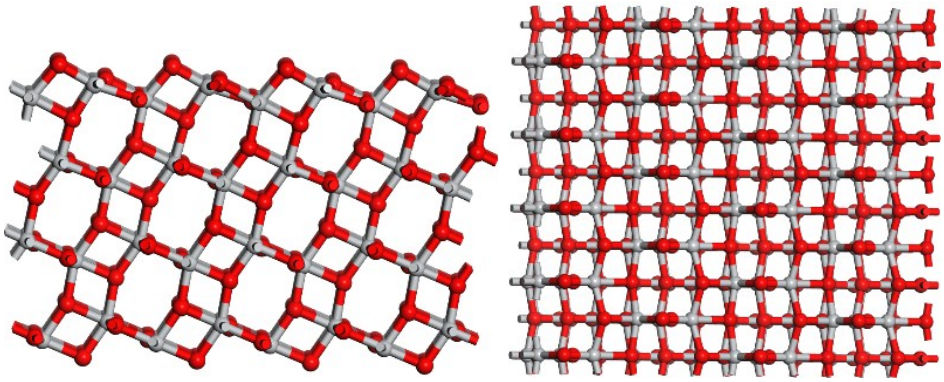

Side view Top view

Fig. S8. The side and top view of anatase (101) surface

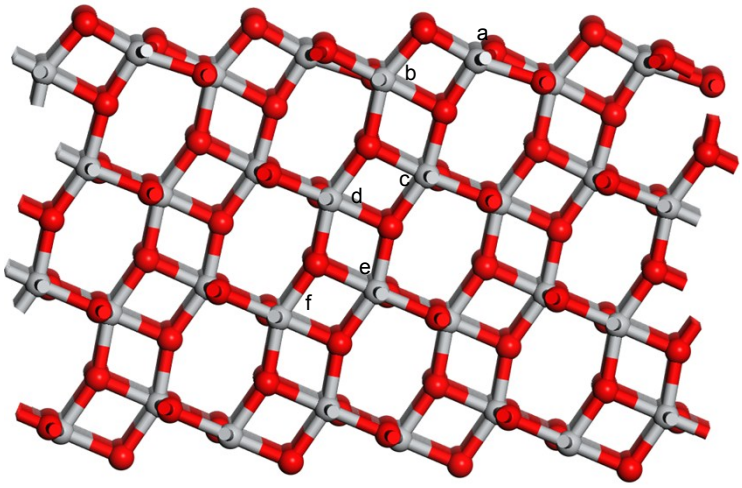

Sites	*E*	Δ*E*
a	-3702.05	0.36
b	**-3702.41**	**0.00**
c	-3702.28	0.13
d	-3702.39	0.01
e	-3702.36	0.05
f	-3702.37	0.04

Fig. S9. The image and relative energy (E) of Nb doped TiO_2 (101). **Note:** the more negative E represents the more stable configuration of the structures

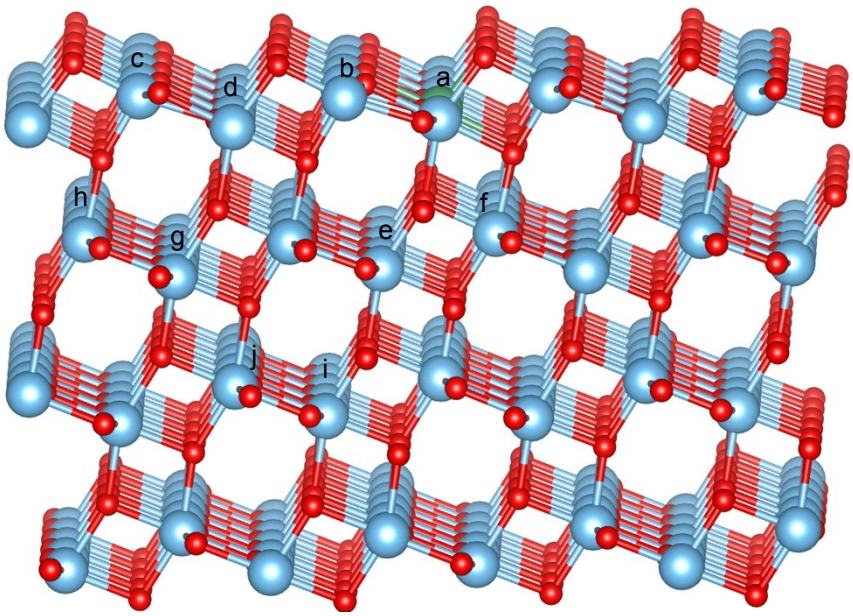

Sites	*E*	Δ*E*
a	-3694.79	1.06
b	**-3695.85**	**0.00**
c	-3694.66	1.19
d	-3695.68	0.17
e	-3694.47	1.38
f	-3694.20	1.65
g	-3694.32	1.53
H	-3694.15	1.70
I	-3694.12	1.73
J	-3694.09	1.76

Fig. S10. The image and relative energy (E) of Pb substitution in Nb doped TiO_2 (101)

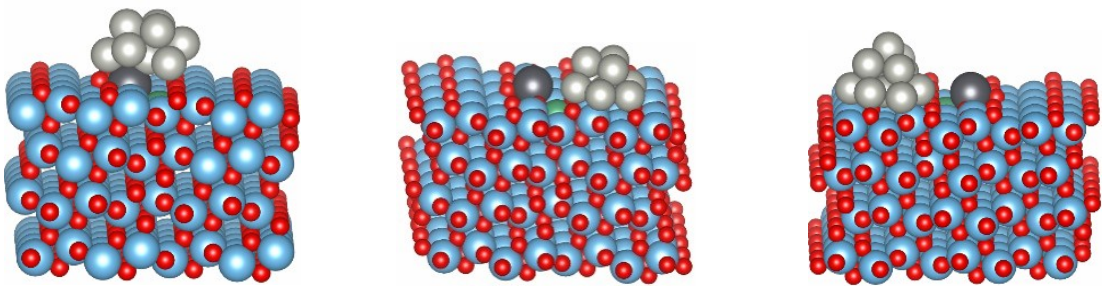

a (on Pb and Nb dopants)	**b (near Nb dopants)**	**c** (far dopants)
E: -3736.30	**-3737.60**	-3736.72
ΔE : 1.30	**0.00**	1.12

Fig. S11. The image of the Pd_{10} loading on the Nb-Pb codoped TiO_2 (101)

Based on the above analysis, a relatively small range of formation energies of structures with different substitution positions and loading distances indicate high stability of the Nb-Pb codoped and Pd loading TiO_2 structures. For subsequent study of electronic properties, the most stable configuration of Nb-Pb codoped and Pd loading TiO_2 was chosen as the **Fig. S11b.**

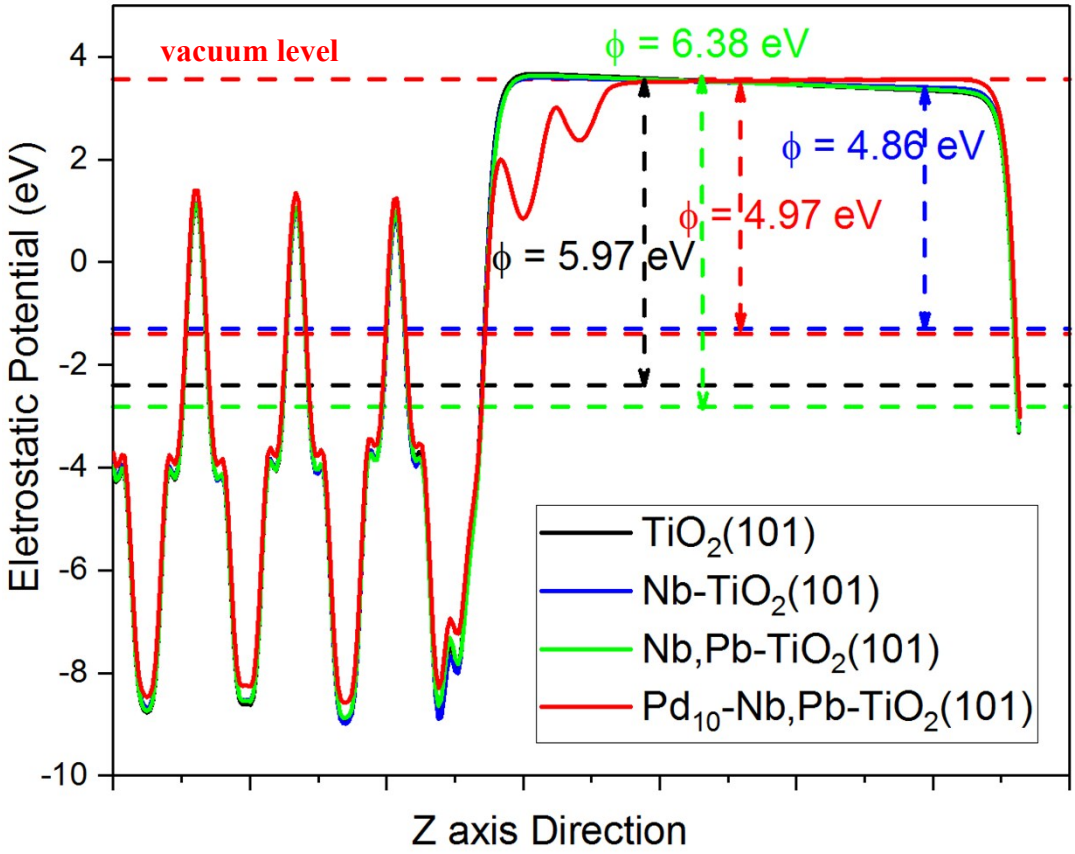

Fig. S12. The calculated work function of the samples